JCTC Journal of Chemical Theory and Computation

Topological Analysis of the Interactions between Organic Molecules and Co(Ni)MoS Catalytic Active Phases

Emmanuel Krebs,[†,‡] Bernard Silvi,*[,†] and Pascal Raybaud[§]

Laboratoire de Chimie Théorique, Université Pierre et Marie Curie, (UMR-CNRS 7616), 4 Place Jussieu 75252-Paris cédex, France, IFP Direction Chimie et Physico-Chimie Appliquées, 1 & 4 Av. de Bois-Préau, 92852 Rueil-Malmaison cédex, France, and IFP Direction Catalyse et Séparation, Rond-point de l'échangeur de Solaize, BP3 69360 Solaize, France

Received August 19, 2008

Abstract: The adsorption modes of toluene, 2,3-dimethylbut-1-ene, and 2-methylthiophene on the edges of Co(Ni)MoS nanocrystallites has been investigated with the ELF topological approach of chemical bonding. The chemisorbed modes are characterized by the formation of bonding basins linking the substrate to the catalytic sites. The electronic rearrangements within the substrate are discussed. It is shown that a unique electronic descriptor, namely the metallic atomic basin contribution to the substrate ELF basins, provides a sizable correlation with the interaction energy.

1. Introduction

Hydrotreating reactions catalyzed by γ-alumina-supported Co(Ni)MoS catalysts are playing a key role in industrial refining in order to produce cleaner fuels.[1] The Co(Ni)MoS active phase has been widely studied by many experimental[2] and theoretical techniques[3] to provide an accurate description of the catalyst at an atomic scale. The active phase consists of MoS_2 nanocrystallites with a deformed hexagonal 2D-morphology and exposing two active edges, the so-called "S-"and "M-edges".[3,4] In order to increase the activity of the MoS_2 active phase, promoters (Co or Ni) are substituted to Mo atoms located at both edges of the crystallites. The edge energies and atomic structures depend on the sulfiding conditions and to the promoter coverage, and they have been investigated by "first principles" calculations based on periodic density functional theory in numerous previous works.[3−8] Furthermore, it has been shown that the 2D-morphology (and as a result the type of edge sites) depends on the nature and proportion of promoter (Co or Ni) at edges.[9] Depending on the reaction conditions, different typical proportions of the promoter can be stabilized at the edges, which induces different types of local arrangement of the metal and sulfur atoms. Hence, specific conditions can be found where the edges are fully covered by the promoters and other cases where the edges are only partially decorated by Co or Ni atoms, with some neighboring Mo atoms. These different local environments are strongly suspected to influence the catalytic reactivity[10] and the selectivity.[11] Many DFT works have also performed adsorption energy calculations of sulfur organic molecules including thiophene and dibenzothiophene[4,12−17] and nitrogen organic molecules.[3,18,19] A recent DFT study has focused on the determination of the most stable adsorption mode of 2,3-dimethylbut-1-ene and 2-methylthiophene on the Co(Ni)MoS edges.[11] These molecules represent two important classes of sulfur organic and olefin compounds present in hydrotreatment reactions of gasoline. This study has provided an interpretation of the selective hydrodesulfuration of 2-methylthiophene based on the adsorption energy calculated values. It is the subject of the present work to provide a more fundamental understanding based on the nature of the chemical bonding of these energy results. We will thus furnish a theoretical description of the electronic interaction between the adsorbed molecules and the active edges. In addition, aromatics are an important family of hydrocarbons molecules also present in hydrotreating reactions catalyzed by Co(Ni)MoS catalysts.[10,20] In order to achieve a coherent

* Corresponding author e-mail: silvi@lct.jussieu.fr.
† Université Pierre et Marie Curie.
‡ IFP Direction Chimie et Physico-Chimie Appliquées.
§ IFP Direction Catalyse et Séparation.

10.1021/ct800344r CCC: $40.75
Published on Web 02/06/2009

comparison including this family of reactant, the present work will investigate the stable adsorption configuration of toluene on CoMoS edges and also provide an electronic analysis of its chemical bonding on the same edge sites.

The characterization of the bonding interactions between the adsorbed molecules and the active sites is a key for the *chemical* understanding of the catalytic process. The analysis of the bonding is usually carried out by either rather crude orbital-based methods or qualitative descriptions of electron density maps. Only few published works use more rigorous topological techniques such the AIM,[21] the topology of the electrostatic potential,[22] or the ELF approach.[23] Aray et al. have recently published interesting analysis carried out with AIM[24−27] and also with the electrostatic potential.[28−31]

To our knowledge, the topological ELF approach has already been used in surface science to characterize the adsorption of CO and CN^- on surfaces,[32] F centers on MgO surfaces,[33] and the adsorption of Pd atoms on MgO, Al_2O_3, and SiO_2 surfaces.[34]

This paper aims to provide a description of the bonding of adsorbed toluene, 2,3-dimethylbut-1-ene, and 2-methylthiophene molecules on promoted MoS_2 edges based on the ELF topological analysis in order to get a deeper insight on:

(1) the qualitative and quantitative aspects of bond formation and charge transfers between the catalyst and the substrate,

(2) the evolution of the bonds of the adsorbed species with respect to the uncomplexed molecules.

For this purpose we have selected a representative sample of four toluene, thirteen 2,3-dimethylbut-1-ene, and fourteen 2-methylthiophene adsorption modes on which the ELF topological analysis has been carried out.

2. Methodology

2.1. The Topological Analysis of Electron Distribution Functions. One of the goals of the topological analysis of electron distribution functions is to provide a partition of the geometrical space occupied by the chemical system of interest (molecule, aggregate, polymer, 1−3 D periodic system) into adjacent nonoverlapping volumes called basins. These basins are thought as corresponding to chemical entities such as atoms in molecules, atomic cores, bonds, or lone pairs. The partition is achieved with the help of a rigorous mathematical method, namely the Dynamical System Theory (see Abraham et al.),[35,36] applied to the gradient vector field of a quantum mechanically well defined local function of the electron distribution which carries the chemical information.

The choice of the local function is determined by the type of description of the bonding. The one electron density $\rho(r)$ has its regular maxima at nuclei where the Coulombic electron nucleus attractive potential tends to infinity. Therefore, one nuclear attractor and one basin is associated to each atom. As non-nuclear attractors are exceptions in molecular system at equilibrium,[37] the basins of the electron density attractors are called atomic basins and constitute the backbone of the AIM theory of R. F. W. Bader.[21] In order to recover a description close to Lewis's bonding picture, it is necessary to consider another local function able to locate the boundary between two regions where opposite spin pairs are localized. This can be achieved by the Electron Localization Function (ELF) which was originally designed by Becke and Edgecombe to identify "localized electronic groups in atomic and molecular systems".[38] It relies, through its kernel, on the laplacian of the conditional same spin pair probability scaled by the homogeneous electron gas kinetic energy:

$$\chi_\sigma(r) = \frac{D_\sigma(r)}{D_\sigma^0(r)} \tag{1}$$

in which

$$D_\sigma(r) = \tau_\sigma(r) - \frac{1}{4}\frac{(\rho_\sigma(r))^2}{\rho_\sigma(r)}$$

appears to be the difference of the actual definite positive kinetic energy $\tau_\sigma(r)$ and the von Weizsäcker kinetic energy functional,[39] whereas

$$D_\sigma^0(r) = \frac{3}{5}(6\pi^2)^{2/3}\rho_\sigma^{5/3}(r)$$

is the kinetic energy density of the homogeneous electron gas. This formulation led Savin to propose an interpretation of ELF in terms of the local excess kinetic energy because the Pauli repulsion enabled its calculation from Kohn−Sham orbitals.[40−42] Orbital-based interpretations of ELF have been proposed by Burdett[43] and more recently by Nalewajski et al.[44] who considered the nonadditive interorbital Fisher information. Another route pioneered by Dobson[45] explicitly considers the pair functions. It has been independently developed by Kohout et al.[46,47] and by one of us,[48] allowing the extension of ELF to correlated wave functions.[49]

The topological partition of the ELF gradient field[23,50] yields basins of attractors which can be thought as corresponding to atomic cores, bonds, and lone pairs. The core basins surround nuclei with atomic number $Z > 2$ and are labeled C(A) where A is the atomic symbol of the element. The valence basins are characterized by the number of atomic valence shells to which they participate, or in other words by the number of core basins with which they share a boundary. This number is called the synaptic order.[51] Thus, there are monosynaptic, disynaptic, trisynaptic basins, and so on. Monosynaptic basins, labeled V(A), correspond to the lone pairs of the Lewis model, and polysynaptic basins to the shared pairs of the Lewis model. In particular, disynaptic basins, labeled V(A, X) correspond to two-center bonds, trisynaptic basins, labeled V(A, X, Y) to three-center bonds, and so on. The valence shell of a molecule is the union of its valence basins. As hydrogen nuclei are located within the valence shell, they are counted as a formal core in the synaptic order because hydrogen atoms have a valence shell. For example, the valence basin accounting for a C−H bond is labeled V(C, H) and called protonated disynaptic. The valence shell of an atom, for example A, in a molecule is the union of the valence basins whose label lists contain the element symbol A. This description recovers Lewis's picture of the bonding[52,53] and provides very suggestive graphical representations of molecular systems. A quantitative analysis

is further achieved by integrating the electron density and the pair functions over the volume of the basins yielding both basin populations:

$$\bar{N}(\Omega_A) = \int_{\Omega_A} \rho(r)\mathrm{d}r \quad (2)$$

and the corresponding covariance matrix[54] which measures the quantum mechanical uncertainties of the electron distribution and supports a phenomenological interpretation in terms of weighted mesomeric structures.[55]

Combining the ELF and AIM approaches, Raub and Jansen[56] have introduced a bond polarity index defined as:

$$p_{XY} = \frac{\bar{N}[V(X, Y)|X] - \bar{N}[V(X, Y)|Y]}{\bar{N}[V(X, Y)|X] + \bar{N}[V(X, Y)|Y]} \quad (3)$$

where $\bar{N}[V(X, Y)|X]$ denotes the contribution of the X atom to the population of the V(X, Y) basin, i.e., the integrated density over the intersection of the V(X, Y) ELF basin and the atomic basin of atom X.

In the context of the ELF analysis, the concept of domain is very important because it enables definition of chemical units within a system and to characterization of valence domains belonging to a given chemical unit. The sole gradient dynamical system mathematical properties do not provide the whole set of definitions necessary to describe the bonding in molecules, and therefore some other mathematically based approaches are required for this purpose. The topological concept of domain has been introduced in chemistry by P. Mezey in order to recognize functional groups within organic molecules.[57] Generalized to ELF isovalues this concept has proved to be an efficient "generator" of clear definitions. Any subset of the molecular space bounded by an external closed isosurface $\eta(r) = f$ is a domain. A f-localization domain is such a subset with the restriction that each point satisfies $\eta(r) > f$. A localization domain surrounds at least one attractor; in this case it is called irreducible. If it contains more than one attractor, it is reducible. An irreducible domain is a subset of a basin whereas a reducible one is the union of subsets of different basins. Except for atoms and linear molecules, the irreducible domains are always filled volumes whereas the reducible ones can be either filled volumes or hollowed volumes.

Upon the increase of the value of $\eta(r)$ defining the bounding isosurface, a reducible domain split into several domains each containing less attractors than the parent domain. The reduction of localization occurs at turning points which are critical points of index 1 located on the separatrix of two basins involved in the parent domain. Ordering these turning points (localization nodes) by increasing $\eta(r)$ enables tree-diagrams to be built reflecting the hierarchy of the basins. Three types of domains can be distinguished according to the nature of the attractors within them. A core domain contains the core attractor(s) of a given atom, a valence domain contains only valence attractors, and a composite domain contains both valence and core attractors. For any system there exists low values of $\eta(r) = f$ defining a unique composite parent domain. The successive reductions of localization will split this parent domain. Every child which is a composite domain corresponds to one or more chemical species. A chemical unit is the union of the basins of the last appearing composite domain of a branch provided it is a filled volume. This concept which has been successfully used for hydrogen bonding[58] enables characterization of physisorption vs chemisorption. In the former case the first reduction yields two composite domains corresponding to the substrate and to the surface, respectively, whereas in the latter case the parent domain splits into core domains encompassed by a hollowed volume.

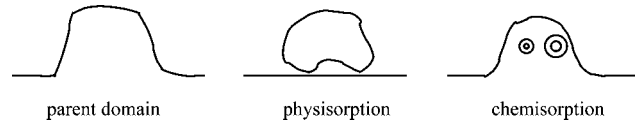

Figure 1. Bifurcation scheme of physisorption and chemisorption.

The case of adsorption is illustrated by Figure 1: the parent domain corresponding to a low ELF value contains both the substrate and the surface; when the isovalue defining the contour is raised, it splits either into two filled domains (physisorption) or becomes a hollowed volume encompassing the core domains (chemisorption). In the same manner as for the hydrogen bonding case where the ELF analysis is able to discriminate weak, medium, and strong H-bonds, several situations may occur for chemisorption according to the changes of the number of basins and of the synaptic order of some of them during the process. In a first case, very similar to physisorption, neither the number of basins nor the synaptic order varies. The topology of the substrate−surface system is just the addition of the topologies of the moieties which preserve their own valence shells, and the chemical interaction mostly consists of the increase of the electron density fluctuation of adjacent basins belonging to these valence shells, in other words an increase of the delocalization. The number of basins may remain constant whereas at least one synaptic order changes when one of the fragments behaves as a Lewis acid, in this case a monosynaptic basin (lone pair) of the other partner becomes disynaptic and therefore forms a dative bond. In the last case, the covalent chemisorption, the number of basins increases by the appearance of disynaptic basins between the substrate and the surface.

2.2. The ELF Analysis of Large Systems. In our group, the analysis of the ELF function is usually carried out with the TopMoD software[59] which has been initially designed to treat rather small-sized systems. In the first step, the program evaluates ELF over a three-dimensional regular grid whose recommended step size is on the order of 0.1−0.2 bohr. Larger step sizes may seriously downgrade the reliability of the results. In the second step, the program assigns the grid points to the different basins: from each grid point a trajectory is built until it leads to a region already assigned to an attractor basin. This procedure is robust if the whole set of attractors are located within the box. Because the computational cost increases as the cube of the box dimension, the ELF analysis of large systems becomes rapidly unfeasible. Moreover, the useful information provided by the calculation represents a small amount of the output. In order to overcome these difficulties we use a trick enabling us to safely carry out the analysis on a subset of atoms. For a given point, the contribution of the given localized basis function

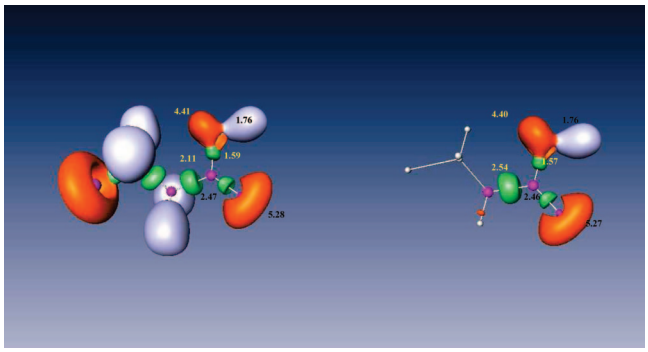

Figure 2. Localization domains and basin populations of the acid functional group of CH_2ClCH_2COOH. Left: full calculation; right: partial calculation. Color code: magenta = core, red = monosynaptic, blue = protonated disynaptic, green = disynaptic.

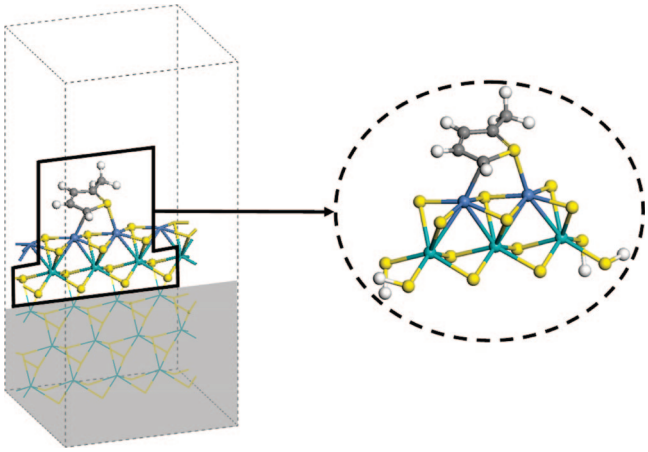

Figure 3. Example of the construction of a cluster (right) starting from a periodic supercell (left).

to both ELF and $\rho(r)$ dramatically depends upon the distance between the origin of the basis function and the point. Because of the exponential decay of the basis functions, contributions arising from those typically centered farther than 5 bohrs from the point are very small and thus can be neglected. Therefore, the basis functions centered on atoms which are not the nearest neighbors of those of the subset of interest can be legitimately discarded, yielding an auxiliary basis set to be actually used by the ELF analysis.

Figure 2 displays the localization domains and basin population of the functional group of CH_2ClCH_2COOH. The approximate calculation provides an almost identical aspect of the domains in the region of interest; moreover, the error on the populations is at most 0.02 e, the expected accuracy of the integration, except for the V(C,C) basin which belongs to the boundary zone.

2.3. Computational Methods. The ab initio calculations of molecules have been performed at the hybrid Hartree−Fock density functional B3LYP level[60−63] with the Gaussian 03 software.[64] The geometries and energetics of the adsorbed species have been optimized in periodic slab calculations carried out with the VASP plane waves periodic code.[65,66] The slab size is given in Figure 3. For more details on the slab model, the reader could refer to refs 9 and 11. The different edge structures for the CoMoS and NiMoS catalysts

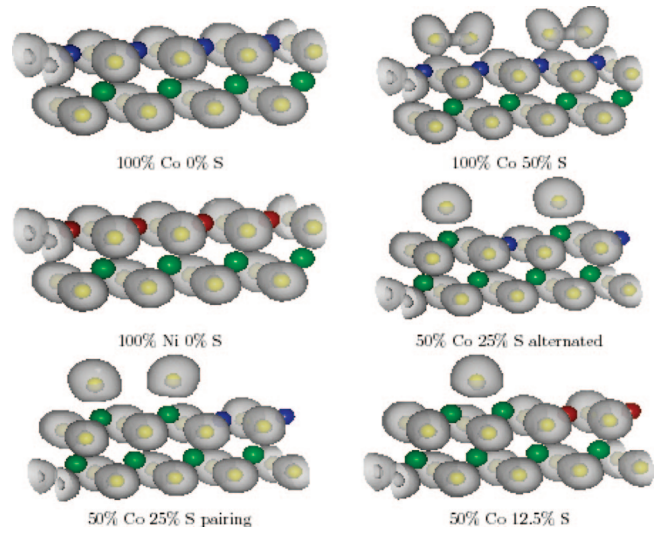

Figure 4. η = 0.7 Localization domains of the M edge structures after geometry optimization for the two promoter contents and the most stable sulfur coverage (yellow balls: S; green balls: Mo; blue balls: Co; brown ball: Ni).

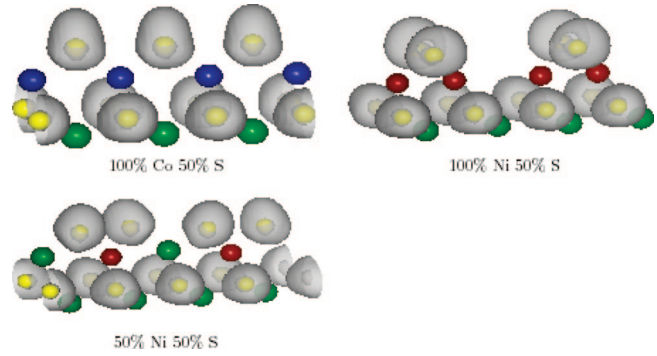

Figure 5. η = 0.7 Localization domains of the S edge structures after geometry optimization for the two promoter contents and the most stable sulfur coverage (yellow balls: S, green balls: Mo; blue balls: Co; brown ball: Ni).

are reported in Figures 4 and 5. The energy values as used later are defined as:

$$\Delta E_{\text{int}} = E(\text{mol} + \text{edge}) - E(\text{edge}_{\text{def}}) - E(\text{mol}_{\text{def}}) \quad (4)$$

$$\Delta E_{\text{def}}(\text{mol}) = E(\text{mol}_{\text{def}}) - E(\text{mol}) \quad (5)$$

$$\Delta E_{\text{def}}(\text{edge}) = E(\text{edge}_{\text{def}}) - E(\text{edge}) \quad (6)$$

$$\Delta E_{\text{ads}} = E(\text{mol} + \text{edge}) - E(\text{edge}) - E(\text{mol}) = \Delta E_{\text{int}} + \Delta E_{\text{def}}(\text{edge}) + \Delta E_{\text{def}}(\text{mol}) \quad (7)$$

where E(mol + edge) is the total energy of the molecule adsorbed on the edge, E(edge) the energy of the free edge (respectively, molecule for mol), and $E(\text{edge}_{\text{def}})$ the energy of the edge (respectively molecule for mol) deformed when the molecule is adsorbed on it. For adsorption energy calculations on the periodic slab, the GGA-PW91 functional[67] has been used. The cutoff energy is 500 eV, while the convergence criteria on forces is fixed at 0.05 eV/Å. For a more detailed description on the conditions for the periodic DFT calculations of 2,3-dimethylbut-1-ene and 2-methylthiophene adsorptions, the reader may also refer to ref 11

Representative clusters have been built from the periodic geometries (see Figure 3) and the B3LYP calculations performed with the standard 3−21G basis set.[68−73] The analysis of the ELF function has been carried out with the TopMoD program developed in the Laboratoire de Chimie Théorique de l'Université Pierre et Marie Curie.[59] The accuracy of the integrated densities is on the order of 0.02 e. The ELF isosurfaces have been visualized with the Amira 3.0 software.[74]

3. Results and Discussion

The adsorption modes on M- and S-edges are governed by the interactions between the metallic sites of the catalyst, which play the role of electrophilic centers, with the nucleophilic sites of the adsorbed molecules. Figures 4 and 5 display the ELF = 0.7 localization domains of some of the most important optimized M- and S-edges structures for the Co(Ni)MoS system calculated by VASP. In the M-edge the metal sites are above the average surface plane and therefore easily accessible by any nucleophilic part of the adsorbed molecule. However, at partial sulfur coverage the sulfur atoms may play a repulsive role and therefore partially hamper the chemisorption. On S-edges, the metal sites are much less accessible and the adsorption will therefore be much more difficult unless the shape of the nucleophilic center of the ad-molecule fits the available voids between sulfur atoms. Among other possibilities are the substitution of a sulfur of the edge by a heteroatom of the molecule and the displacement of sulfur atoms of the edge to create an accessible metal site.

Three types of nucleophilic sites can be encountered with respect to their dimensionality:

(1) polygonal sites correspond to electron delocalization within an aromatic ring; the adsorbed molecule is expected to lie in a plane parallel to the edge direction either on top of a metal site or in a bridged position between two,

(2) bond sites correspond to the interaction of a multiple bond with a metallic site; they are expected to be less subject to geometrical constraint,

(3) substitution sites in which an atom of the ad-molecule is involved in the coverage of the edge.

According to Pauling's electronegativity scale[75,76] Co should have a greater electrophilic character than Ni and Mo whereas in Allred and Rochow's scale[77] molydenum is the less electronegative. However, an indication of the electrophilic character of the metallic centers can be deduced from the ELF and QTAIM population analysis carried out in the present work. As a general rule, core basin populations are rather stable: the averaged core population of Co, Ni, and Mo are calculated to be 25.24 ± 0.05, 26.27 ± 0.06, and 39.72 ± 0.09, respectively, whereas larger standard deviations are calculated for the AIM atomic populations. According to these values, the stronger interactions are expected with molybdenum in agreement with Allred and Rochow's electronegativity.

Different types of bonding between the edge and the molecules are expected. They are named η_i-MM′ for both toluene (Figure 6) and 2-methylthiophene (Figure 7), where

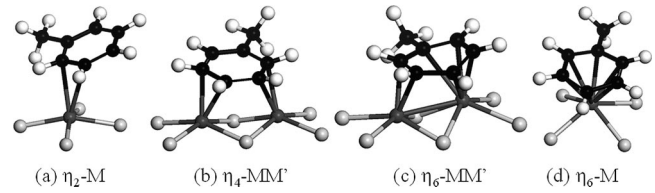

Figure 6. Views of toluene adsorption modes. (Black balls: C; dark gray balls: edge site (Mo, Co, or Ni); light gray balls: S).

i is the number of atoms supposed to be linked to the metallic edge sites (M and M′ = Mo, Co, Ni). The sulfur atom of the thiophene molecule is always bonded to M. The nomenclature used for 2,3-dimethybut-1-ene is given in Figure 8.

3.1. Toluene Adsorption. It is first interesting to notice that the sum of the deformation energies (molecule+edge) is greater than 0.8 eV for the configurations strongly bound to the edge (η_i-MM′ for $i \geq 4$), whereas it is only about 0.42 eV for the less attached η_2-Co configuration. This is due to the very low molecule deformation energy for this last configuration compared to the others, while the deformation energy of the edge remains constant. Nevertheless, this configuration is the less favorably adsorbed one, considering interaction or adsorption energies.

The ELF localization domains of the free toluene molecule and of three of its adsorption modes are displayed in Figure 9 whereas the population analysis is reported in Table 1. The nucleophilic part of the toluene molecule is clearly delocalized over the aromatic ring, and therefore one can expect that the adsorption will take place preferentially on the M-edge with the molecular plane parallel to the edge direction. The "on top" adsorption over a Mo atom is expected to yield a six-coordinated complex (η_6) which could be characterized by the presence of six disynaptic basins between the metal and each carbon of the cycle. In fact there are only two disynpatic V(Mo, C) basins in the adsorbed species which involve the ipso and para carbons. The sum of the integrated densities over these basins is 1.18 e. It results from a density transfer from the $C_{ipso}-C_{ortho}$ and $C_{meta}-C_{para}$ bonds which lowers the population of the related disynaptic basins to ca. 2.3 e whereas the V(C_{ortho}, C_{meta}) population is slightly increased by 0.2 e with respect to the free molecule. Indeed, there is no destablizing loss of aromaticity because the delocalization remains unchanged for these latter bonds. However, the four other bonds are substantially elongated and therefore the distance between the metal and the ortho and meta carbon are slightly larger than those involving the ipso and para ones which is consistent with an effective η_2 structure. These bond elongations may be due to a strong electron delocalization between the Mo site and the toluene ring. In fact, the contribution of the Mo to the V(C, C) basins (0.23 e) has been found to be slightly larger than its contributions to the V(C, Mo) basins (0.19 e).

In the η_4 mode, two Co atoms are in bridging positions below the $C_{ortho}-C_{meta}$ and $C_{meta}-C_{para}$ bonds located on the same side with respect to the $C_{ipso}-C_{para}$ direction. Four V(Co, C) disynaptic basins are formed between the Co atoms

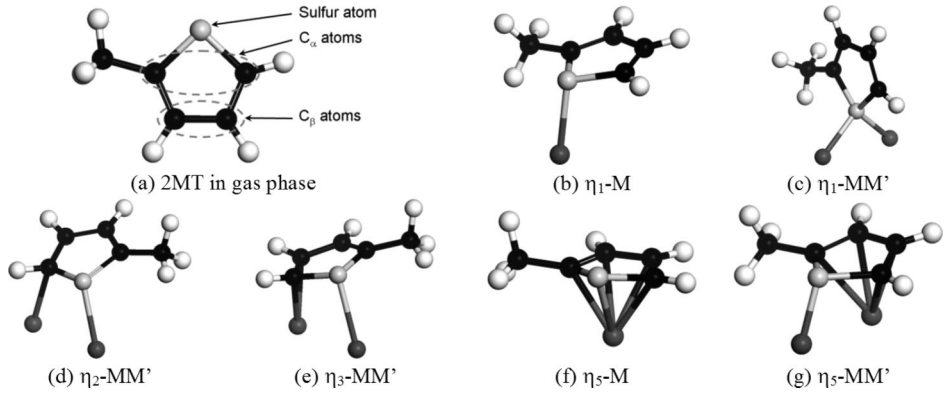

Figure 7. View of different modes of adsorption of 2-methylthiophene. (Black balls: C; dark gray balls: edge site (Mo, Co, or Ni); light gray balls: S).

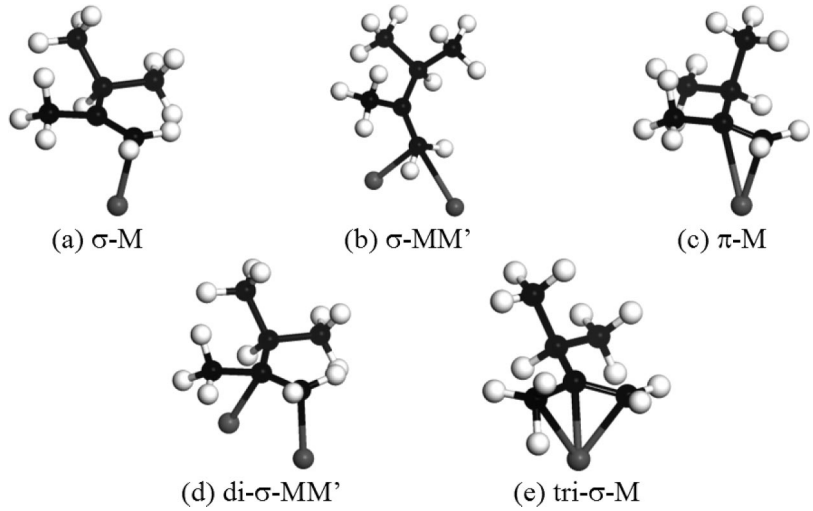

Figure 8. View of different modes of adsorption of 2,3-dimethylbut-ene. (Black balls: C; dark gray balls: edge site (Mo, Co, or Ni)).

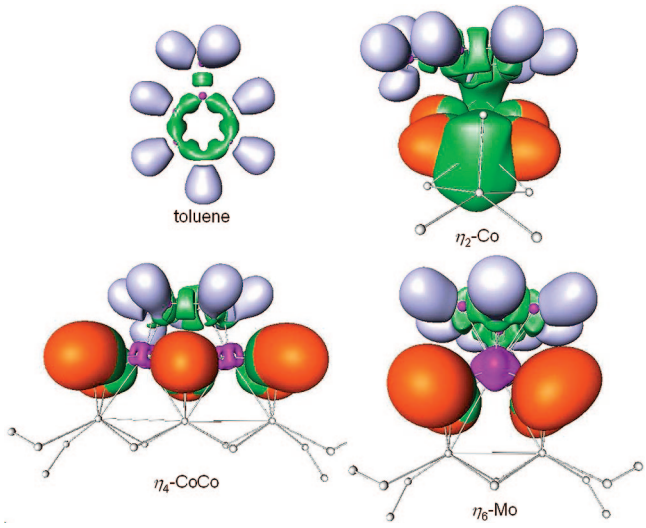

Figure 9. ELF = 0.7 localization domains of toluene showing the aromatic ring. ELF = 0.75 localization domains of the η_2, η_4, and η_6 adsorption modes.

and the nearest carbons, and therefore the η_4 bonding mode can be unambiguously assigned to this adsorption mode. The populations of the V(Co, C) basins range between 0.30 and 0.46 e and mostly come from all the C−C bonds of the cycle except the $C_{ipso}-C_{ortho}$ one which belong to the other half-plane. The basin populations are almost independent of the sulfur coverage, and the stability difference between the 0 and 12.5% edges should be due to the repulsion arising from the sulfur lone pairs. Similar to this, the Co contribution to the V(C, Co) and V(C,C) basins (0.33 e) is exactly the same for both edges.

In the η_2 mode, the Co atom is located below the $C_{ortho}-C_{meta}$ bond. The adsorption process yields disynaptic basins between Co and C_{ortho} and in the case of the 25% sulfur coverage investigated here an interaction of the second C_{ortho} with two linked S atoms because the related V(S, S) basin has a trisynaptic character. However, with respect to the increase of the number of basins due to adsorption, this structure should be named η_1 rather than η_2. Although the V(Co, C_{ortho}) population is low (0.36 e), the changes in the V(C, C) population are rather large; for example, the V(C_{ortho}, C_{meta}) basin loses 1.14 e with respect to the free molecule. Nevertheless, Co contributes to this bond up to 0.02 e over a total of 0.07 e. The calculated interaction energies are first consistent with the Allred and Rochow electronegativity scale and in second place with the number of disynaptic V(C, M) basins.

3.2. 2,3-Dimethylbut-1-ene Adsorption. The detailed results obtained on the adsorption modes and energies of

Table 1. Population Analysis, Deformation, Adsorption, and Interaction Energies (eV) of Toluene Molecule Adsorbed on M-Edge Sites[a]

	CoMoS M-edge: coverage (%M−%S)				
adsorp mode	free	50 (a)−12.5 η_6-Mo	100−0 η_4-CoCo	50 (p)−12.5 η_4-CoCo	50 (p)−25 η_2-Co
$\bar{N}$ [V(Mo, C_{ipso})]		0.53			
$\bar{N}$ [V(Co, C_{ortho})]			0.30	0.33	0.36
$\bar{N}$ [V(Co, C_{meta})]			0.45	0.46	
			0.30	0.39	
$\bar{N}$ [V(Co, C_{para})]			0.43	0.41	
$\bar{N}$ [V(Mo, C_{para})]		0.65			
$\bar{N}$ [V(S, S, C_{ortho})]					3.11
$\bar{N}$ [V(C_{ipso}, C_{ortho})]	2.81	2.35	2.35	2.32	2.44
			3.17	3.18	2.93
$\bar{N}$ [V(C_{ortho}, C_{meta})]	2.82	3.01	2.45	2.47	1.87
			2.33	2.27	2.49
$\bar{N}$ [V(C_{meta}, C_{para})]	2.79	2.28	2.12	2.11	2.60
			2.43	2.44	2.92
$\sum\bar{N}$ [V(C, M)]		1.18	1.48	1.59	0.36
$\sum\bar{N}$ [V(C, X)M][b]		0.42	0.33	0.33	0.07
ΔE_{def} (mol)		0.20	0.45	0.49	0.06
ΔE_{def} (edge)		0.53	0.41	0.34	0.36
ΔE_{ads}		−1.73	−0.63	−0.65	0.00
ΔE_{int}		−2.46	−1.68	−1.48	−0.42

[a] Except for η_6-Mo, the toluene molecule loses the C_s symmetry. In the coverage entry, a means alternated, and p means pairing (see Figure 4). [b] X = C, M; M = Mo, Co.

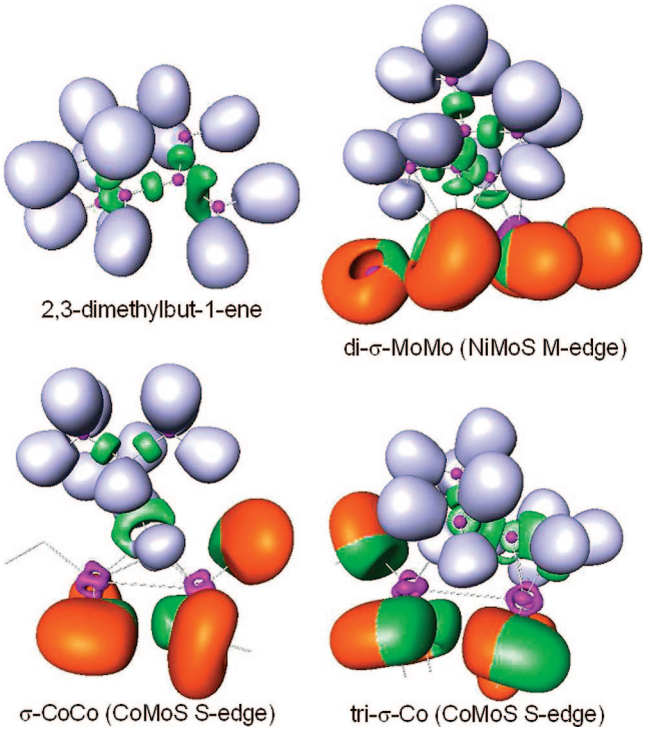

Figure 10. ELF = 0.7 localization domains of 2,3-dimethylbut-1-ene; ELF = 0.80 localization domains of the di-σ-MoMo, σ-CoCo (CoMoS S-edge), and tri-σ-Co adsorptions modes.

2,3-dimethylbut-1-ene (as well as 2-methylthiophene) are reported in ref 11. In what follows, we focus on the ELF analysis and the deformation energy values derived from the adsorption modes found in our previous study. The ELF localization domains of the free 2,3-dimethylbut-1-ene molecule and of three of its adsorption modes are displayed in Figure 10 whereas the population analysis is reported in Tables 2 and 3. The nucleophilic center is the terminal C═C double bond, the approach of which toward a metallic site is not hampered less by repulsions due to sulfur atoms than to those due to the aromatic ring of toluene. Therefore adsorptions on both M- and S-edges are thermodynamically possible.

3.2.1. Adsorption on the M-Edge. The two adsorption configurations on Mo sites (π-Mo and di-σ-MoMo) present significant energetic differences with respect to Co and Ni sites. Even if the molecule is strongly deformed (ΔE_{def} (mol) > +0.9 eV), the adsorption energies are the most exothermic ones (ΔE_{ads} < −1.5 eV) because of highly exothermic interaction energies (ΔE_{int} < −2.5 eV).

Adsorption configurations on Co sites are all presenting a sum of deformation energies lower or equal to +0.9 eV, whereas on Ni, it is less than +0.4 eV. As a consequence, even if adsorption energies on Co and Ni sites are in the same range (between 0 and −0.8 eV), interaction energies are always more exothermic on Co sites (between −0.98 and −1.41 eV) than on Ni sites (above −0.75 eV). In this case, we observe an anticorrelation between the interaction energies and the deformation energies of the molecules for all configurations.

The geometries of the adsorption modes on the CoMoS M-edge sites are all with the double bond "on top" of a metal atom. At low sulfur coverage, 12.5%, there are two disynaptic basins V(M, C(1)) and V(M, C(2)) linking the olefin to the metal M. The population of these basins is on the order of 1.2 with Mo and of 0.5 with Co in agreement with the respective electronegativities of these metals. The V(C(1), C(2)) population decreases from 3.73 in the free molecule to 2.50 in the adsorbed molecule. Such adsorption site should be referred as η_2 rather than as σ and π. At larger sulfur coverage, the adsorbed molecule is linked to the surface by only one disynaptic basin (η_1 mode), the population of which is always less than 0.8 e. The V(C(1), C(2)) population, ∼2.72 e, is slightly larger than that of the η_2 mode.

On the NiMoS M-edge, the strongest adsorption occurs for a Ni coverage of 50% without sulfur, the C(1) and C(2) carbons are on top of two Mo atoms, and the olefin molecule is linked to the surface by a disynaptic V(Mo, C(2)) and a trisynaptic V(Mo, C(1), Mo′) basin both with populations larger than 1 e (1.3 and 1.64, respectively). Accordingly, the C(1)−C(2) bond loses its double bond character because its population is lowered to 1.84 e. This density transfers are expected to favor the hydrogenation of the olefin. When the Ni coverage is increased to 100%, the larger electronegativity of Ni hampers the formation of two basins and only the V(Ni, C(1)) basin with a rather small population of 0.64 e is observed. The C−Ni bond lengths are indeed larger (2.23 Å and 2.66 Å) than the C−Mo ones (from 2.12 Å to 2.37 Å). The population of V(C(1), C(2)), 2.70, is close to those calculated for the adsorption in the CoMoS structures. Finally, rather small sulfur coverage hampers the formation of any disynaptic basin. Nevertheless, a stable complex can be formed. Although this adsorption mode belongs to physisorption, the surface and the ad-molecule share the same valence shell because the ELF bifurcation value is 0.24. The

Table 2. Population Analysis, Deformation, Adsorption, and Interaction Energies (eV) of 2,3-Dimethylbut-1-ene Molecule Adsorbed on M-Edge Sites[a]

	CoMoS M-edge: coverage (%M−%S)					
adsorp mode	free	50 (a)−25 σ-Co	50 (a)−12.5 π-Mo	50 (p)−25 σ-Co	50 (p)−12.5 π-Co	100−25 π-Co
$\bar{N}$ [V(Co, C(1))]		0.79		0.79	0.65	0.66
$\bar{N}$ [V(Mo, C(1))]			1.26			
$\bar{N}$ [V(Co, C(2))]					0.36	
$\bar{N}$ [V(Mo, C(2))]			1.20			
$\bar{N}$ [V(C(1), C(2))]	3.73	2.72	2.50	2.71	2.50	2.73
$\sum\bar{N}$ [V(C, M)]		0.79	2.46	0.79	1.01	0.66
$\sum\bar{N}$ [V(C, X)|M][b]		0.15	0.48	0.16	0.24	0.25
ΔE_{def} (mol)		0.27	0.92	0.28	0.43	0.37
ΔE_{def} (edge)		0.63	0.13	0.34	0.26	0.24
ΔE_{ads}		−0.08	−1.54	−0.43	−0.72	−0.73
ΔE_{int}		−0.98	−2.59	−1.05	−1.41	−1.34

	NiMoS M-edge: coverage (%M−%S)		
adsorp mode	50 (p)−12.5 σ-Ni	50 (p)−0 di-σ-MoMo	100−0 σ-Ni
$\bar{N}$ [V(Ni, C(1))]			0.64
$\bar{N}$ [V(Mo, C(2))]		1.30	
$\bar{N}$ [V(Mo, C(1), Mo′)]		1.64	
$\bar{N}$ [V(C(1), C(2))]	3.56	1.84	2.70
$\sum\bar{N}$ [V(C, M)]	0.00	2.94	0.64
$\sum\bar{N}$ [V(C, X)|M][b]	0.08	0.63	0.14
ΔE_{def} (mol)	0.07	1.85	0.20
ΔE_{def} (edge)	0.06	0.25	0.15
ΔE_{ads}	−0.13	−1.94	−0.40
ΔE_{int}	−0.26	−4.04	−0.75

[a] In the coverage entry, a means alternated, and p means pairing (see Figure 4). [b] X = C, M; M = Mo, Co, Ni.

Table 3. Population Analysis, Deformation, Adsorption, and Interaction Energies (eV) of 2,3-Dimethylbut-1-ene Molecule Adsorbed on S-Edge Sites[a]

	CoMoS S-edge: coverage (%M−%S)		NiMoS S-edge: coverage (%M−%S)		
adsorp mode	100−50 σ-CoCo	100−37.5 tri-σ-Co	50 (a)-50 π-Mo	50 (a)-37.5 di-σ-NiMo	100−37.5 σ-NiNi
$\bar{N}$ [V(Co, C(1))]	0.99	0.87			
$\bar{N}$ [V(Mo, C(1))]			0.86		
$\bar{N}$ [V(Ni, C(1))]				1.34	0.66
$\bar{N}$ [V(Co, C(2))]		0.71			
$\bar{N}$ [V(Mo, C(2))]			0.69	0.91	
$\bar{N}$ [V(C(1), C(2))]	2.78	2.50	2.44	2.05	2.96
$\sum\bar{N}$ [V(C, M)]	0.99	1.58	1.55	2.25	0.66
$\sum\bar{N}$ [V(C, X)|M][b]	0.18	0.43	0.37	0.48	0.12
ΔE_{def} (mol)	0.16	0.37	0.54	1.37	0.10
ΔE_{def} (edge)	1.01	1.29	2.08	1.48	0.14
ΔE_{ads}	0.72	−0.51	0.81	0.16	−0.12
ΔE_{int}	−0.45	−2.18	−1.81	−2.69	−0.35

[a] In the coverage entry, a means alternated, and p means pairing (see Figure 5). [b] X = C, M; M = Mo, Co, Ni.

population of the double bond is noticeably perturbed because it is lowered by 0.17 e with respect to the free molecule.

As a general rule for equivalent adsorption modes, the Co and Ni contributions to the V(C, M) and V(C, C) basins have very similar values independent of the V(C, M) populations whereas the contribution of Mo is significantly larger.

3.2.2. Adsorption on the S-Edge. On this edge, we can distinguish the sites of adsorption of the molecule by comparing deformation energies: adsorption on pure Ni sites leads to a sum of deformation energies lower to +0.3 eV whereas it comprises between +1.1 and +1.7 eV on pure Co sites and above +2.6 eV on sites with at least one Mo atom. Hence, some resulting adsorption energies are endothermic, even if all interaction energies are exothermic. It is important to underline that the S-edge deformation energies are generally higher than those of the M-edge, because of the energy cost for the relaxation of S-atoms observed on the S-edge.

The olefin is linked to the S-edge by two disynaptic basins either when the sulfur coverage is less than 50% (CoMoS) or if a Mo site is involved (NiMoS). The thermodynamically favored adsorption, di-σ-NiMo, contains at the same time a molybdenum site and a sulfur coverage less than 50%. The double bond forms a bridge between the Ni and Mo sites; therefore, the two disynaptic basins connect different metal cores to different carbons, and their populations are 1.34 and 0.91 for V(Ni, C(1)) and V(Mo, C(2)), respectively. Consequently, the population of the V(C(1), C(2)) basins is lowered to a single bond value, i.e. 2.05 e. The two other

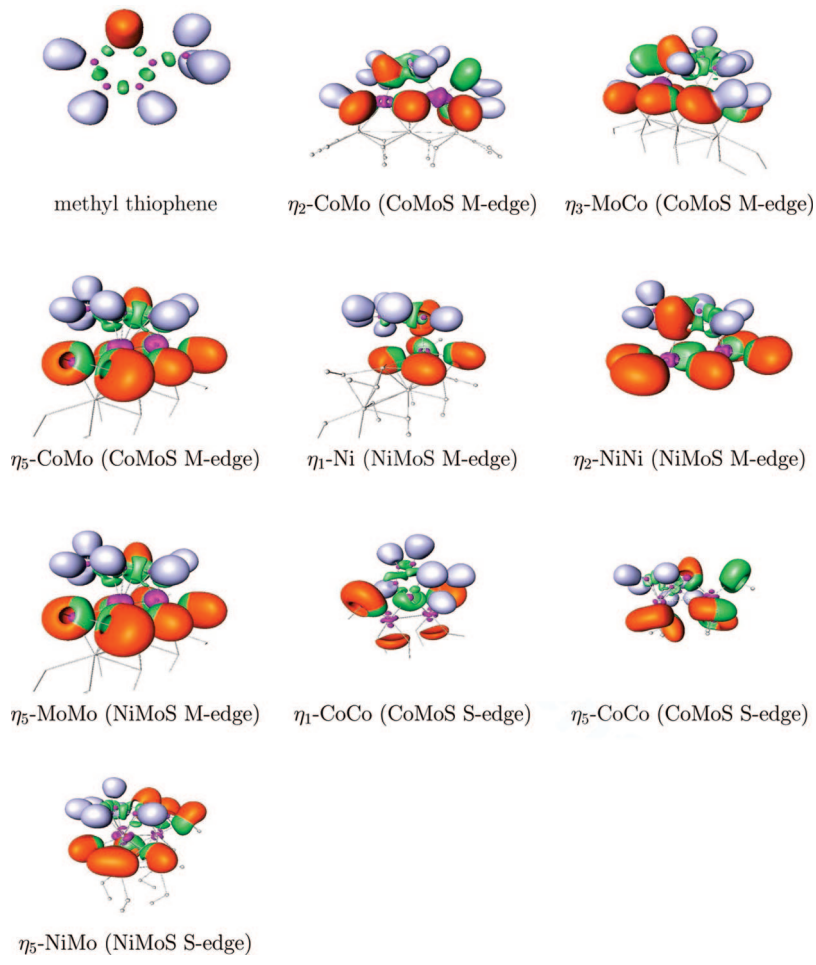

Figure 11. ELF = 0.8 localization domains of 2-methylthiophene; ELF = 0.75 localization domains of the η_2-CoMo, η_3-MoCo, η_5-CoMo, η_1-Ni, η_2-NiNi, η_5-MoMo, η_1-CoCo η_5-CoCo, and η_5-NiMo adsorptions modes.

adsorption modes involving two disynaptic basins, the so-called tri-σ-Co and π-Mo, are electronically very similar: on the one hand, the basin population V(M, C(1)) and V(M, C(2)) are very close independent of the nature of the metal (0.87 and 0.86 for V(M, C(1)), 0.71 and 0.69 for V(M, C(2)); on the other hand, the V(C(1), C(2)) population has almost the same values as the other π modes on M-edge. The difference of the interaction energies is consistent with the metal contributions to the olefin basins.

The V(M, C(1)) populations, metal contributions to the olefin basins, and interaction energies of the σ-MM modes are in line with the electronegativities of Co and Ni.

3.3. 2-Methylthiophene Adsorption. Figure 11 displays the localization domains of free and adsorbed 2-methylthiophene whereas the ELF population analysis is reported in Tables 4, 5, and 6. The nucleophilic regions of 2-methylthiophene are, on the one hand, the heterocycle which has an aromatic character and, on the other hand, the sulfur lone pairs which can form a dative bond with the metallic sites.

3.3.1. Adsorption on the M-Edge. First, we observe that the sum of deformation energies depends on the type of mode, i.e. number of supposed interacting bonds between the molecule and the edge: the deformation energies increased with i in the η_i-mode. Consequently, a ranking is observed for interaction energies: greater than −0.6 eV for η_1 modes, between −0.6 and −1.3 eV for η_2 modes, around −1.8 eV for η_3 modes, and below −3.0 eV for η_5 modes. As for the olefin molecules, we observe an anticorrelation

Table 4. Population Analysis, Deformation, Adsorption, and Interaction Energies (eV) of 2-Methylthiophene Molecule Adsorbed on CoMoS M-Edge Sites[a]

	CoMoS M-edge: coverage (%M−%S)				
adsorp mode	free	50 (a)−25 η_2-CoMo	50 (a)−12.5 η_5-CoMo	50 (p)−25 η_3-MoCo	50 (p)−12.5 η_3-CoCo
$\bar{N}$ [V(Co, S)]		2.07	2.05		
$\bar{N}$ [V(Co′, S)]					2.26
$\bar{N}$ [V(Mo, S)]				1.98	
$\bar{N}$ [V(Co, C(5))]				1.06	1.28
$\bar{N}$ [V(Co, C(4))]				0.52	0.66
$\bar{N}$ [V(Mo, C(5))]		1.10	0.93		
$\bar{N}$ [V(Mo, C(4))]			0.45		
$\bar{N}$ [V(Mo, C(3))]			0.28		
$\bar{N}$ [V(Mo, C(2))]			1.08		
$\bar{N}$ [V(S, C(5))]	1.29	1.21	1.20	1.23	1.16
$\bar{N}$ [V(S, C(2))]	1.31	1.42	1.24	1.30	1.31
$\bar{N}$ [V(C(4), C(5))]	3.82	2.58	2.37	2.34	2.36
$\bar{N}$ [V(C(3), C(4))]	2.21	2.38	2.46	2.14	2.09
$\bar{N}$ [V(C(2), C(3))]	3.91	3.44	2.53	3.70	3.73
$\Sigma\bar{N}$ [V(C, M)]		1.10	2.74	1.58	1.94
$\Sigma\bar{N}$ [V(Y, X)IM][b]		0.21	0.53	0.34	0.47
ΔE_{def} (mol)		0.22	0.54	0.40	0.42
ΔE_{def} (edge)		0.49	0.47	0.43	0.27
ΔE_{ads}		−0.54	−2.31	−0.90	−1.19
ΔE_{int}		−1.25	−3.32	−1.74	−1.88

[a] In the coverage entry, a means alternated, and p means pairing (see Figure 4). [b] Y = C, S; X = C, S, M; M = Mo, Co.

Table 5. Population Analysis, Deformation, Adsorption, and Interaction Energies (eV) of 2-Methylthiophene Molecule Adsorbed on NiMoS M-Edge Sites[a]

	NiMoS M-edge: coverage (%M−%S)				
adsorp mode	50 (p)−12.5 η_2-MoNi	50 (p)−12.5 η_1-Ni	50 (p)−0 η_5-MoMo	100−0 η_2-NiNi	100−0 η_1-Ni
$\bar{N}$ [V(Ni, S)]		1.95		1.98	1.86
$\bar{N}$ [V(Mo, S)]	1.97		1.74		
$\bar{N}$ [V(Ni, C(5))]	0.87			0.85	
$\bar{N}$ [V(Mo, C(5))]			1.66		
$\bar{N}$ [V(Mo′, C(4))]			0.51		
$\bar{N}$ [V(Mo′, C(3))]			0.49		
$\bar{N}$ [V(Mo, C(2))]			1.44		
$\bar{N}$ [V(S, C(5))]	1.31	1.31	1.13	1.30	1.32
$\bar{N}$ [V(S, C(2))]	1.35	1.32	1.10	1.37	1.32
$\bar{N}$ [V(C(4), C(5))]	2.62	3.66	1.96	2.62	3.62
$\bar{N}$ [V(C(2), C(3))]	3.53	3.75	2.33	3.52	3.71
$\bar{N}$ [V(C(3), C(4))]	2.31	2.31	2.55	2.32	2.32
$\sum\bar{N}$ [V(C, M)]	0.87	0.0	4.10	0.85	0.00
$\sum\bar{N}$ [V(Y, X)IM][b]	0.22	0.08	0.70	0.24	0.11
ΔE_{def} (mol)	0.13	0.00	1.29	0.09	0.02
ΔE_{def} (edge)	0.27	0.05	0.26	0.19	0.11
ΔE_{ads}	−0.26	−0.23	−2.90	−0.45	−0.41
ΔE_{int}	−0.66	−0.28	−4.45	−0.73	−0.54

[a] In the coverage entry, a means alternated, and p means pairing (see Figure 4). [b] Y = C, S; X = C, S, M; M = Mo, Ni.

between the interaction energy and the deformation energy of the molecule. This trend explains why there is no direct link between adsorption energies and the bonding mode. Furthermore, deformation energies of the thiophene molecule are in general smaller than those of the olefin.

At low sulfur coverage, both CoMoS and NiMoS edges are able to adsorb 2-methylthiophene through an η_5 mode characterized by one V(M, S) basin and four V(Mo, C) ones. The population of the V(Mo, C) basins are on the order of 1 and 1.5 e for the CoMoS and NiMoS edges, respectively, whereas the two other V(Mo, C) basins have populations on the order of 0.5 e or less. Although the population of the V(M, S) basin is larger on the CoMoS than on the NiMoS edge, the interaction of the latter is larger in absolute value, indicating that the adsorption is controlled by the V(Mo, C) populations. An equalization of the V(C, C) basin populations of the cycle with respect to the free molecule is observed.

The η_3 adsorption modes occur on the CoMoS edge. They involve the sulfur and the C(4) and C(5) carbons. The interaction between Co and the former carbon is weaker than that between Co and the latter, the ratio of the populations of V(Co, C(5)) and V(Co, C(4)) being on the order of 2. The interaction being geometrically asymmetric with respect to S, only V(C(4), C(5)) undergoes a significant variation of its population.

The η_2 modes are electronically very similar, although the V(M, C(5)) population is larger for the CoMoS than for the NiMoS because it involves a Mo site in the CoMoS rather than a Ni site in the NiMoS. It is worth noting that the V(C(2), C(3)) is more perturbed than for η_3 modes.

The η_1 modes of NiMoS clearly belong to physisorption, as the bifurcation value of ELF is less than 0.2 for both.

3.3.2. Adsorption on the S-Edge. As for the M-edge, we can distinguish the adsorption modes by the sum of their deformation energies: for η_1 modes it is less than 1.5 eV whereas it is more than 2.0 eV for η_5 modes. Consequently, even if there is no direct link with adsorption energies, interaction energies of η_5 modes are always more exothermic than for η_1 modes (less than −2.5 eV vs more than −1.5 eV). Furthermore, for the 2-methylthiophene molecule as well as for the olefin, it appears that the deformation energy of the S-edge is always larger than that of the M-edge.

Two adsorption modes are possible on the S-edge: either the highly coordinated η_5 or the η_1 in which the 2-methylthiophene structure substitutes a sulfur edge atom. The bond properties of η_5-CoCo are very similar to those of the M-edge η_5-CoMo. The η_5-NiMo is in fact an η_4 mode involving a trisynaptic bridging V(Ni, S, Mo) basin. The equalization of the V(C, C) basin trend is weaker than for the true η_5 mode.

In the η_1 modes, the lone pairs of the sulfur atoms form two dative bonds with two neighboring metallic sites, the 2-methylthiophene sulfur occupying a "substitution" site. The populations within the heterocycle are very weakly perturbed and the contribution of the metallic sites is always larger than for the M-edge η_1 mode. This contribution as well as the interaction energy absolute value is larger for η_1-CoCo than for η_1-NiNi and η_1-MoNi. Similarly, the η_1-CoCo S−Co bonds (2.21 Å) are smaller than η_1-NiNi and η_1-MoNi S−Ni (2.32 Å to 3.01 Å) and S−Mo bonds (2.58 Å).

3.4. Correlation between Metallic Site Contributions and Interaction Energy. The calculation of the basin population provides a basis for the understanding of the electronic scheme during the adsorption of the three molecules (toluene, 2-methylthiophene, and 2,3-dimethylbut-1-ene) on both edges. As a first insight, it appears clear that even if the adsorption energy (defined according to eq 7) is the most representative for the thermodynamic process, this quantity cannot be correlated with any of the electronic descriptors provided by the basin population analysis. According to eq 7, the adsorption energy contains the contribution of three distinct terms: the interaction energy, and the deformation energies of the molecule and of the edge. According to the values reported in Table 1−6 and described in the previous section, it appears clear that the deformation energies cannot be neglected and strongly depend on the molecules, on the adsorption mode, and on the edge considered. Hence, it is impossible to find a direct correlation between ELF basin populations and the adsorption energy. In contrast, it can be reasonably expected that the V(X, M) basins shared between the atoms (X) of the adsorbed molecule and the metallic sites of the catalyst (M) contribute to the interaction energy. Therefore, a first descriptor, $\sum\bar{N}$[V(X, M)], is built by summing the populations of the V(X, M) basins. For toluene and 2,3-dimethylbut-1-ene, the values of this index are reported in the $\sum\bar{N}$[V(C, M)] entry of Tables 1−3 whereas for dimethylthiophene the V(M, S) populations have to be added to $\sum\bar{N}$[V(C, M)]. The plot of this sum as a function of the interaction energy (Figure 12) enables us to distinguish the thiophene molecule from the olefin and toluene molecules. The population of the V(S, M) basin is indeed a strong contributor to the sum of the population of the V(X, M) basins. This may qualitatively explain why the methylthiophene molecule is more strongly

Table 6. Population Analysis, Deformation, Adsorption, and Interaction Energies (eV) of 2-Methylthiophene Molecule Adsorbed on S-Edge Sites[a]

	CoMoS S-edge: coverage (%M−%S)		NiMoS S-edge: coverage (%M−%S)		
adsorp mode	100−50 η_1-CoCo	100−37.5 η_5-CoCo	50 (a)−50 η_1-MoNi	50 (a)−37.5 η_5-NiMo	100−37.5 η_1-NiNi
$\bar{N}$ [V(Co, S)]	2.28	2.26			
$\bar{N}$ [V(Co′, S)]	2.62				
$\bar{N}$ [V(Mo, S)]			2.15		
$\bar{N}$ [V(Ni, S)]			2.52		2.33
$\bar{N}$ [V(Ni′, S)]					2.44
$\bar{N}$ [V(Ni, S, Mo)]				4.65	
$\bar{N}$ [V(Co, C(5))]		0.96			
$\bar{N}$ [V(Co, C(2))]		0.98			
$\bar{N}$ [V(Co, C(4))]		0.47			
$\bar{N}$ [V(Co, C(3))]		0.47			
$\bar{N}$ [V(Mo, C(5))]				1.13	
$\bar{N}$ [V(Mo, C(2))]				1.02	
$\bar{N}$ [V(Mo, C(4))]				0.35	
$\bar{N}$ [V(S, C(5))]	1.22	1.20	1.27	1.22	1.27
$\bar{N}$ [V(S, C(2))]	1.22	1.16	1.28	1.24	1.27
$\bar{N}$ [V(C(4), C(5))]	3.69	2.40	3.68	2.40	3.67
$\bar{N}$ [V(C(2), C(3))]	3.77	2.53	3.75	2.56	3.76
$\bar{N}$ [V(C(3), C(4))]	2.13	2.25	2.20	2.78	2.17
$\sum\bar{N}$ [V(C, M)]	0.00	2.88	0.00	2.52	0.00
$\sum\bar{N}$ [V(Y, X)|M][b]	0.31	0.60	0.13	0.55	0.19
ΔE_{def} (mol)	0.04	0.73	0.03	0.22	0.03
ΔE_{def} (edge)	1.00	1.45	1.40	3.06	0.41
ΔE_{ads}	−0.24	−1.37	0.35	0.41	−0.59
ΔE_{int}	−1.28	−3.55	−1.08	−2.87	−1.03

[a] In the coverage entry, a means alternated, and p means pairing (see Figure 5). [b] Y = C, S; X = C, S, M; M = Mo, Co, Ni.

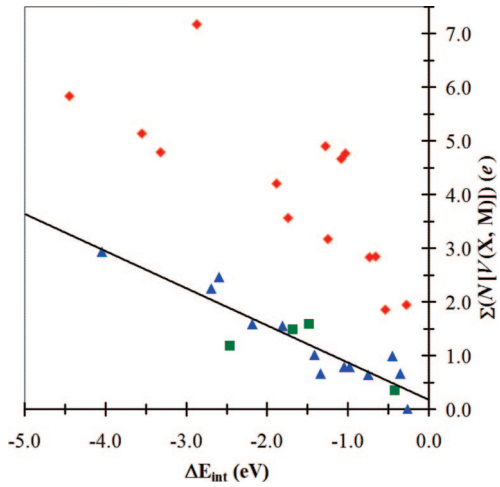

Figure 12. Sum of the populations $\sum\bar{N}$[V(X, M)] vs interaction energy. Green square: toluene; blue triangle: 2,3-dimethylbut-1-ene adsorption; red lozenge: 2-methylthiophene adsorption. (X = S, C; M = Mo, Co, Ni).

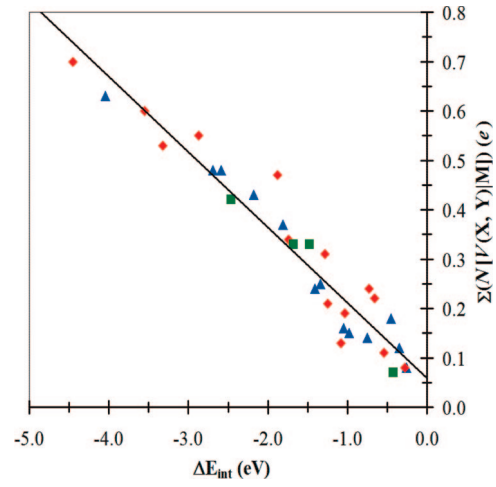

Figure 13. Sum of metal contributions $\sum\bar{N}$ [V(X,M) | M] vs interaction energy. Green square: toluene; blue triangle: 2,3-dimethylbut-1-ene adsorption; red lozenge: 2-methylthiophene adsorption. (X = S, C; M = Mo, Co, Ni).

stabilized. In contrast, for the olefin and the toluene, the unique contribution comes from the V(C, M) basins. However, as also revealed by Figure 12, the sum of the populations of V(X, M) basins cannot quantitatively unify the trend in interaction energies for the three molecules. For 2-methylthiophene, the ELF populations are overestimated because of the contribution of some nonbonding part in the V(S, M) population. A unique electronic descriptor valid for the whole sample of studied systems would be nevertheless very useful. In Figure 13, it appears that such a descriptor can be proposed if we consider the $\sum\bar{N}$[V(X, Y)|M] quantity. In this case, the value of the correlation coefficient, −0.96, validates this descriptor as relevant for the interaction energy.

The $\sum\bar{N}$[V(X, Y)|M] quantity (also reported in Tables 1−3) is calculated by adding the metal AIM atomic basin contributions to the V(C, M), V(C, S), V(C,C), and V(M, S) populations. In other words, it is the integrated density over the intersection of the V(C, M), V(C, S), V(C,C), and V(M, S) basins and the atomic basin of the metal. Hence, it clearly accounts for the electron density shared between the catalyst and the adsorbed molecule. The sum of the metal atomic basin contributions to the substrate ELF basins accounts for the partial covalent character of the interaction and, therefore, is found to be correlated with the electronic interaction energies of the molecules with metallic sites. This interesting correlation gives a rational explanation based on

the ELF analysis of the interaction energy term contributing to the resulting adsorption energy. This evaluates the pure contribution of the chemical bonding between the adsorbed molecule and the metallic sites as also contained in the interaction energy, when the other effects such as deformation energies of the edges and molecules are subtracted.

4. Conclusions

The conclusions which can be drawn from the present work concern both technical and chemical aspects of computational chemistry. From a methodological viewpoint, our results demonstrate the feasibility of ELF analysis on rather large systems related to surface chemistry. On the one hand, the calculation of the ELF function and of the integrated densities with a cluster model in which the atomic positions have been optimized at a periodic level is a unique possibility until a periodic code is available for plane waves. Fortunately, this approach yields realistic results at least for the adsorbed molecule subset. On the second hand, the computational effort is significantly reduced by the atom selection procedure which has the additional advantage of simplifying the graphical representations.

The chemical pieces of information provided by the ELF analysis mostly concern the nature of the interactions in terms of bond formation between the catalyst and the adsorbed molecule. In the case of physisorption, such as for the 2-methylthiophene η_1 modes on the NiMoS M-edge, the topology of the catalyst + substrate is just the sum of their topologies. The chemisorption is characterized at least by the increase of the synaptic order of a monosynaptic basin, i.e. V(S) becomes V(S, M) in the 2-methylthiophene adsorption, or by the formation of new polysynaptic basins. The number of disynaptic basins linking the substrate to the metallic site may differ from that expected from a purely geometrical coordination as is the case for the η_6 adsorption mode of toluene for which only two disynaptic basins connect the ipso and para carbons to the molybdenum. The ELF analysis should be therefore helpful to improve the nomenclature used to name the adsorption modes, making it more precise. A proposal of the form η_n (M), $\eta_{n'}$ (M′),..., where the subscripts n, n',..., indicate the number of bonds made by the metallic sites M, M′,..., with the substrate improves the implicit description of the bonding properties of each site. In our opinion such nomenclature is less confusing than that used initially in this paper. The same π-Co name is used for two adsorption modes of the olefin on the CoMoS edge, giving rise to one and two V(C, M) basins; naming them η_2 (Co) and η_1 (Co) enables a better differentiation.

The ELF analysis also sheds light, in a chemical language, on the electronic rearrangements in the substrate, indicating which bonds are activated. For example, our results show that the 2-methylthiophene C–S bonds are weakened in the η_5 adsorption modes and more particularly in the η_5-MoMo one on the NiMoS M-edge which also corresponds to the largest absolute value of the interaction energy.

Finally, we propose an exhaustive analysis of the different energy components involved in the adsorption energy: the interaction energy and the deformation energy of the molecule and of the edge. In particular, because of nonnegligible deformation energies of the molecule and of the edge, it can be better understood why the adsorption energy cannot correlate with the ELF electronic descriptor. In contrast, the interaction energy is the most representative of the electronic exchange taking place between the substrate and the adsorbate and thus exhibits a good correlation with the ELF descriptor.

References

(1) Prins, R. Hydrotreating Reactions. In *Handbook of Heterogeneous Catalysis*; Ertl, G.; Knözinger, H.; Weitkamp, J., Eds.; Wiley-VCH: Weinheim, Germany, 1997; vol. *4*, p 1908.

(2) Topsøe, H.; Clausen, B. S.; Massoth, F. E. Catalyst Characterization. In *Hydrotreating Catalysis Science and Technology*; Anderson, J. R., Boudart, M., Eds.; Springer-Verlag: Berlin, Germany, 1996; vol. *11*, p 29.

(3) Raybaud, P. Understanding and predicting improved sulfide catalysts: Insights from first principles modeling. *Appl. Catal. A* **2007**, *322*, 76.

(4) Paul, J.-F.; Cristol, S.; Payen, E. Computational studies of (mixed) sulfide hydrotreating catalysts. *Catal. Today* **2008**, *130*, 139.

(5) Raybaud, P.; Hafner, J.; Kresse, G.; Kasztelan, S.; Toulhoat, H. Structure, Energetics, and Electronic Properties of the Surface of a Promoted MoS_2 Catalyst: An ab Initio Local Density Functional Study. *J. Catal.* **2000**, *190*, 128.

(6) Byskov, L. S.; Nørskov, J. K.; Clausen, B. S.; Topsøe, H. DFT Calculations of Unpromoted and Promoted MoS_2-Based Hydrodesulfurization Catalysts. *J. Catal.* **1999**, *187*, 109.

(7) Schweiger, H.; Raybaud, P.; Toulhoat, H. Promoter Sensitive Shapes of Co(Ni)MoS Nanocatalysts in Sulfo-Reductive Conditions. *J. Catal.* **2002**, *212*, 33.

(8) Sun, M.; Nelson, A. E.; Adjaye, J. On the incorporation of nickel and cobalt into MoS_2-edge structures. *J. Catal.* **2004**, *226*, 32.

(9) Krebs, E.; Silvi, B.; Raybaud, P. Mixed sites and promoter segregation: A DFT study of the manifestation of Le Chatelier's principle for the Co(Ni)MoS active phase in reaction conditions. *Catal. Today* **2008**, *130*, 160.

(10) Gandubert, A. D.; Krebs, E.; Legens, C.; Costa, D.; Guillaume, D.; Raybaud, P. Optimal promoter edge decoration of CoMoS catalysts: A combined theoretical and experimental study. *Catal. Today* **2008**, *130*, 149.

(11) Krebs, E.; Silvi, B.; Daudin, A.; Raybaud, P. A DFT study of the origin of the HDS/HydO selectivity on Co(Ni)MoS active phases. *J. Catal.* **2008**, *260*, 276.

(12) Cristol, S.; Paul, J.-F.; Payen, E.; Bougeard, D.; Hutschka, F.; Clemendot, S. DBT derivatives adsorption over molybdenum sulfide catalysts: a theoretical study. *J. Catal.* **2004**, *224*, 138.

(13) Cristol, S.; Paul, J.-F.; Schovsbo, C.; Veilly, E.; Payen, E. DFT study of thiophene adsorption on molybdenum sulfide. *J. Catal.* **2006**, *239*, 145.

(14) Raybaud, P.; Hafner, J.; Kresse, G.; Toulhoat, H. Adsorption of Thiophene on the Catalytically Active Surface of MoS_2: An Ab Initio Local-Density-Functional Study. *Phys. Rev. Lett.* **1998**, *80*, 1481.

(15) Sun, M.; Nelson, A. E.; Adjaye, J. Adsorption Thermodynamics of Sulfur- and Nitrogen-containing Molecules on NiMoS: A DFT Study. *Catal. Lett.* **2006**, *109*, 133.

(16) Orita, H.; Uchida, K.; Itoh, N. A volcano-type relationship between the adsorption energy of thiophene on promoted MoS_2 cluster-model catalysts and the experimental HDS activity: ab initio density functional study. *Appl. Catal. A* **2004**, *258*, 115.

(17) Weber, T.; van Veen, J. R. A density functional theory study of the hydrodesulfurization reaction of dibenzothiophene to biphenyl on a single-layer NiMoS cluster. *Catal. Today* **2008**, *130*, 170.

(18) Sun, M.; Nelson, A. E.; Adjaye, J. Adsorption and hydrogenation of pyridine and pyrrole on NiMoS: an ab initio density-functional theory study. *J. Catal.* **2005**, *231*, 223.

(19) Sun, M.; Nelson, A. E.; Adjaye, J. First principles study of heavy oil organonitrogen adsorption on NiMoS hydrotreating catalysts. *Catal. Today* **2005**, *109*, 49.

(20) Guernalec, N.; Geantet, C.; Raybaud, P.; Cseri, T.; Aouine, M.; Vrinat, M. Dual Effect of H_2S on Volcano Curves in Hydrotreating Sulfide Catalysis. *Oil Gas Sci. Technol.* **2006**, *61*, 515.

(21) Bader, R. F. W. *Atoms in Molecules: A Quantum Theory*; Oxford Univ.Press: Oxford, Great Britain, 1990.

(22) Gadre, S. R.; Shirsat, R. N. *Electrostatics of Atoms and Molecules*; Hyderabad Universities Press: Hyderabad, India, 2000.

(23) Silvi, B.; Savin, A. Classification of chemical bonds based on topological analysis of electron localization function. *Nature* **1994**, *371*, 683.

(24) Aray, Y.; Rodriguez, J.; Vega, D.; Rodriguez-Arias, E. N. Correlation of the Topology of the Electron Density of Pyrite-Type Transition Metal Sulfides with Their Catalytic Activity in Hydrodesulfurization. *Angew. Chem., Int. Ed.* **2000**, *39*, 3810.

(25) Aray, Y.; Rodriguez, J. Atoms in molecules theory for exploring the nature of the MoS_2 catalyst edge sites. *J. Mol. Catal. A: Chem.* **2007**, *265*, 32.

(26) Aray, Y.; Rodriguez, J.; Vega, D. Laplacian of the Electronic Charge Density and Heat of Adsorption of O_2 and CO Molecules on 3d Transition Metals. *J. Phys. Chem. B* **2000**, *104*, 5225.

(27) Aray, Y.; Rodriguez, J.; Vega, D.; Coll, S.; Rodriguez-Arias, E.; Rosillo, F. Adsorption of Thiophene on the RuS_2 (100) and (111) Surfaces: A Laplacian of the Electronic Charge Density Study. *J. Phys. Chem. B* **2002**, *106*, 13242.

(28) Aray, Y.; Rodriguez, J.; Coll, S.; Rodriguez-Arias, E.; Vega, D. Nature of the Lewis Acid Sites on Molybdenum and Ruthenium Sulfides: An Electrostatic Potential Study. *J. Phys. Chem. B* **2005**, *109*, 23564.

(29) Aray, Y.; Marquez, M.; Rodriguez, J.; Coll, S.; Simon-Manso, Y.; Gonzalez, C.; Weitz, D. Electrostatics for Exploring the Nature of Water Adsorption on the Laponite Sheets' Surface. *J. Phys. Chem. B* **2003**, *107*, 8946.

(30) Aray, Y.; Rodriguez, J.; Coll, D.; Gonzalez, C.; Marquez, M. Exploring the Nature of Wetting by Water of Surfaces of Alkane-Amidethiols Adsorbed on Gold Using the Electrostatic Potential Topology. *J. Phys. Chem. B* **2004**, *108*, 18942.

(31) Aray, Y.; Marquez, M.; Rodriguez, J.; Vega, D.; Simon-Manso, Y.; Coll, S.; Gonzalez, C.; Weitz, D. Electrostatics for Exploring the Nature of the Hydrogen Bonding in Polyethylene Oxide Hydration. *J. Phys. Chem. B* **2004**, *108*, 2418.

(32) Ample, F.; Curulla, D.; Fuster, F.; Clotet, A.; Ricart, J. M. Adsorption of CO and CN^- on transition metal surfaces: a comparative study of the bonding mechanism. *Surf. Sci.* **2002**, *497*, 139.

(33) Mori-Sánchez, P.; Recio, J. M.; Silvi, B.; Sousa, C.; Martín Pendás, A.; Luaña, V.; Illas, F. The rigorous characterization of MgO *F* centers as pseudoatoms. *Phys. Rev. B* **2002**, *66*, 075103.

(34) Gomes, J. R. B.; Illas, F.; Silvi, B. Topological analysis of the metal-support interaction: the case of Pd atoms on oxide surfaces. *Chem. Phys. Lett.* **2004**, *388*, 132.

(35) Abraham, R. H.; Shaw, C. D. *Dynamics: The Geometry of Behavior*; Addison Wesley: Redwood City, CA, 1992.

(36) Abraham, R. H.; Marsden, J. E. *Foundations of Mechanics*; Addison Wesley: Redwood City, CA., 1994.

(37) Martín Pendás, A.; Blanco, M. A.; Costales, A.; Mori Sánchez, P.; Luana, V. Non-nuclear Maxima of the Electron Density. *Phys. Rev. Lett.* **1999**, *83*, 1930.

(38) Becke, A. D.; Edgecombe, K. E. A simple mesure of electron localization in atomic and molecular systems. *J. Chem. Phys.* **1990**, *92*, 5397.

(39) von Weizsäcker, C. F. Zur Theorie der Kermassen. *Z. Phys.* **1935**, *96*, 431.

(40) Savin, A.; Becke, A. D.; Flad, J.; Nesper, R.; Preuss, H.; von Schnering, H. G. A New Look at Electron Localization. *Angew. Chem., Int. Ed. Engl.* **1991**, *30*, 409.

(41) Savin, A.; Jepsen, O.; Flad, J.; Andersen, O. K.; Preuss, H.; von Schnering, H. G. Electron Localization in the Solid-State Structures of the Elements: the Diamond Structure. *Angew. Chem., Int. Ed. Engl.* **1992**, *31*, 187.

(42) Savin, A.; Nesper, R.; Wengert, S.; Fässler, T. F. ELF: The Electron Localization Function. *Angew. Chem., Int. Ed. Engl.* **1997**, *36*, 1809.

(43) Burdett, J. K.; McCormick, T. A. Electron Localization in Molecules and Solids: The Meaning of ELF. *J. Phys. Chem. A* **1998**, *102*, 6366.

(44) Nalewajski, R. F.; Koster, A. M.; Escalante, S. Electron Localization Function as Information Measure. *J. Phys. Chem. A* **2005**, *109*, 10038.

(45) Dobson, J. F. Interpretation of the Fermi hole curvature. *J. Chem. Phys.* **1991**, *94*, 4328.

(46) Kohout, M.; Pernal, K.; Wagner, F. R.; Grin, Y. Electron localizability indicator for correlated wavefunctions. I. Parallel spin pairs. *Theor. Chem. Acc.* **2004**, *112*, 453.

(47) Kohout, M.; Pernal, K.; Wagner, F. R.; Grin, Y. Electron localizability indicator for correlated wavefunctions. I. Anti-parallel spin pairs. *Theor. Chem. Acc.* **2005**, *113*, 287.

(48) Silvi, B. The Spin Pair Compositions as Local Indicators of the Nature of the Bonding. *J. Phys. Chem. A* **2003**, *107*, 3081.

(49) Matito, E.; Silvi, B.; Duran, M.; Solà, M. Electron localization function at the correlated level. *J. Chem. Phys.* **2006**, *125*, 024301.

(50) Häussermann, U.; Wengert, S.; Nesper, R. Localization of Electrons in Intermetallic Phases Containing Aluminium. *Angew. Chem., Int. Ed. Engl.* **1994**, *33*, 2069.

(51) Silvi, B. The synaptic order: a key concept to understand multicenter bonding. *J. Mol. Struct.* **2002**, *614*, 3.

(52) Lewis, G. N. The Atom and the Molecule. *J. Am. Chem. Soc.* **1916**, *38*, 762.

(53) Lewis, G. N. *Valence and the Structure of Atoms and Molecules*; Dover: New York, 1966.

(54) Silvi, B. How topological partitions of the electron distributions reveal delocalization. *Phys. Chem. Chem. Phys.* **2004**, *6*, 256.

(55) Poater, J.; Duran, M. Sol evaluation of electron delocalization in aromatic molecules by means of AIM and ELF topological approaches. *Chem. Rev.* **2005**, *105*, 3911.

(56) Raub, S.; Jansen, G. A quantitative measure of bond polarity from the electron localization function and the theory of atoms in molecules. *Theor. Chem. Acc.* **2001**, *106*, 223.

(57) Mezey, P. G. Quantum chemical shape: new density domain relations for the topology of molecular bodies, functional groups, and chemical bonding. *Can. J. Chem.* **1993**, *72*, 928.

(58) Alikhani, M. E.; Fuster, F.; Silvi, B. What can tell the topological analysis of ELF on hydrogen bonding. *Struct. Chem.* **2005**, *16*, 203.

(59) Noury, S.; Krokidis, X.; Fuster, F.; Silvi, B. Computational tools for the electron localization function topological analysis. *Comput. Chem.* **1999**, *23*, 597.

(60) Becke, A. D. Density-functional thermochemistry. III. The role of exact exchange. *J. Chem. Phys.* **1993**, *98*, 5648.

(61) Becke, A. D. Density-functional exchange-energy approximation with correct asymptotic behavior. *Phys. Rev.* **1988**, *A38*, 3098.

(62) Lee, C.; Yang, Y.; Parr, R. G. Development of the Colle-Salvetti correlation-energy formula into a functional of the electron density. *Phys. Rev.* **1988**, *B37*, 785.

(63) Miehlich, B.; Savin, A.; Stoll, H.; Preuss, H. Results obtained with the correlation energy density functionals of Becke and Lee, Yang and Parr. *Chem. Phys. Lett.* **1989**, *157*, 200.

(64) Frisch, M. J.; Trucks, G. W.; Schlegel, H. B.; Scuseria, G. E.; Robb, M. A.; Cheeseman, J. R.; Montgomery, J. A., Jr.; Vreven, T.; Kudin, K. N.; Burant, J. C.; Millam, J. M.; Iyengar, S. S.; Tomasi, J.; Barone, V.; Mennucci, B.; Cossi, M.; Scalmani, G.; Rega, N.; Petersson, G. A.; Nakatsuji, H.; Hada, M.; Ehara, M.; Toyota, K.; Fukuda, R.; Hasegawa, J.; Ishida, M.; Nakajima, T.; Honda, Y.; Kitao, O.; Nakai, H.; Klene, M.; Li, X.; Knox, J. E.; Hratchian, H. P.; Cross, J. B.; Adamo, C.; Jaramillo, J.; Gomperts, R.; Stratmann, R. E.; Yazyev, O.; Austin, A. J.; Cammi, R.; Pomelli, C.; Ochterski, J. W.; Ayala, P. Y.; Morokuma, K.; Voth, G. A.; Salvador, P.; Dannenberg, J. J.; Zakrzewski, V. G.; Dapprich, S.; Daniels, A. D.; Strain, M. C.; Farkas, O.; Malick, D. K.; Rabuck, A. D.; Raghavachari, K.; Foresman, J. B.; Ortiz, J. V.; Cui, Q.; Baboul, A. G.; Clifford, S.; Cioslowski, J.; Stefanov, B. B.; G. Liu, A. L.; Piskorz, P.; Komaromi, I.; Martin, R. L.; Fox, D. J.; Keith, T.; Al-Laham, M. A.; Peng, C. Y.; Nanayakkara, A.; Challacombe, M.; Gill, P. M. W.; Johnson, B.; Chen, W.; Wong, M. W.; Gonzalez, C.;; Pople, J. A. Gaussian 03, Revision A.1; Gaussian Inc., Pittsburgh PA, 2003.

(65) Kresse, G.; Furthmüller, J. Efficiency of ab-initio total energy calculations for metals and semiconductors using a plane-wave basis set. *Comput. Mater. Sci.* **1996**, *6*, 15.

(66) Kresse, G.; Furthmüller, J. Efficient iterative schemes for ab initio total-energy calculations using a plane-wave basis set. *Phys. Rev. B* **1996**, *54*, 11169.

(67) Perdew, J. P.; Wang, Y. Accurate and simple analytic representation of the electron-gas correlation energy. *Phys. Rev.* **1992**, *B45*, 13244.

(68) Binkley, J. S.; Pople, J. A.; Hehre, W. J. Self-consistent molecular orbital methods. 21. Small split-valence basis sets for first-row elements. *J. Am. Chem. Soc.* **1980**, *102*, 939.

(69) Gordon, M. S.; Binkley, J. S.; Pople, J. A.; Pietro, W. J.; Hehre, W. J. Self-consistent molecular-orbital methods. 22. Small split-valence basis sets for second-row elements. *J. Am. Chem. Soc.* **1982**, *104*, 2797.

(70) Pietro, W. J.; Francl, M. M.; Hehre, W. J.; Defrees, D. J.; Pople, J. A.; Binkley, J. S. Self-consistent molecular orbital methods. 24. Supplemented small split-valence basis sets for second-row elements. *J. Am. Chem. Soc.* **1982**, *104*, 5039.

(71) Dobbs, K. D.; Hehre, W. J. Molecular orbital theory of the properties of inorganic and organometallic compounds. 4. Extended basis sets for third-and fourth-row, main-group elements. *J. Comput. Chem.* **1986**, *7*, 359.

(72) Dobbs, K. D.; Hehre, W. J. Molecular orbital theory of the properties of inorganic and organometallic compounds. 5. Extended basis sets for first-row transition metals. *J. Comput. Chem.* **1987**, *8*, 861.

(73) Dobbs, K. D.; Hehre, W. J. Molecular orbital theory of the properties of inorganic and organometallic compounds. 6. Extended basis sets for first-row transition metals. *J. Comput. Chem.* **1987**, *8*, 880.

(74) Amira 3.0; TGS, Template Graphics Sofware, Inc., San Diego, CA, 2002.

(75) Pauling, L. The Nature of the Chemical Bond. IV. The Energy of Single Bonds and the Relative Electronegativity of Atoms. *J. Am. Chem. Soc.* **1932**, *54*, 3570.

(76) Pauling, L. *The Nature of the Chemical Bond*; Cornell University Press: Ithaca, NY, 1948.

(77) Allred, A. L.; Rochov, E. G. A Scale of Electronegativity Based on Electrostatic Force. *J. Inorg. Nucl. Chem.* **1958**, *5*, 264.

CT800344R